

Theory of quantum entanglement and the structure of two-mode squeezed antiferromagnetic magnon vacuum

D. Wuhrer,^{*} N. Rohling,[†] and W. Belzig[‡]

Fachbereich Physik, Universität Konstanz, D-78457 Konstanz, Germany

Recent investigations of the quantum properties of an antiferromagnet in the spin wave approximation have identified the eigenstates as two-mode squeezed sublattice states. The uniform squeezed vacuum and one-magnon states were shown to display a massive sublattice entanglement. Here we expand this investigation and study the squeezing properties of all sublattice Fock states throughout the magnetic Brillouin zone. We derive the full statistics of the sublattice magnon number with wave number \vec{k} in the ground state and show that magnons are created in pairs with opposite wave vectors, hence, resulting in entanglement of both modes. To quantify the degree of entanglement we apply the Duan-Giedke-Cirac-Zoller inequality and show that it can be violated for all modes. The degree of entanglement decrease towards the corners of the Brillouin zone. We relate the entanglement to measurable correlations of components of the Néel and the magnetization vectors, thus, allowing to experimentally test the quantum nature of the squeezed vacuum. The distinct k -space structure of the probabilities shows that the squeezed vacuum has a nonuniform shape that is revealed through the \vec{k} -dependent correlators for the magnetization and the Néel vectors.

I. INTRODUCTION

In recent years the desire to increase the computational power, together with the need of electronic devices in a suitable size made it necessary for electric circuits to become smaller and smaller [1]. Approaching the size, where quantum effects come into play, it was necessary to come up with new ideas to either limit their influence or use the beneficial effects of their quantum nature.

One of these ideas is the use of spin transport to convey information. In metals [2] or semiconductors [3] spin-transport is achieved by diffusive transport of spin carrying electrons. Interactions between electron spins and permanent magnetic moments in magnetic materials gave then birth to hard drives, based on the giant magnetoresistance [4, 5] or tunnel magnetoresistance [6], as a way to store information.

In insulators, which contain permanent magnetic moments, spin-transport can be mediated by collective, excitations of spins [7–9], so called spin-waves [10–12]. Similar to light waves and photons spin waves constitute superposition of elementary quantized, particle-like excitations, the magnons [13, 14].

Ever since the discovery of 2D materials and the possibility to consistently produce them, they are under extensive investigations [15–21]. Combining or gating single layers opened the door to tailor materials with desired properties. One could then use different 2D materials and combine them in a van der Waals heterostructure [22, 23] to merge their properties or give rise to new ones. Recently magnetic 2D materials joined the zoo of 2D materials [24–27] making it possible to include magnetism into these heterostructures. The so created 2D materials

and their spin transport properties are of great interest for future research and spin information processing.

While some nontrivial properties like Bose-Einstein condensation of magnons or black-hole physics in magnonic transport were reported [28], their quantum nature is subject to a debate since classical explanations were made [29]. Intrinsic quantum features like entanglement were predicted for several magnetic insulators [30–32], that still await an experimental confirmation.

To this end, we want to investigate squeezed magnons as eigenstates of an antiferromagnet (AFM) [33–35], which utilizes the well-known optical concept of squeezing [36] in the domain of antiferromagnetism. Already, squeezed magnons have shown to be the eigenstates of ferromagnets [30, 37] in the presence of dipolar interactions and were discussed in the context of ferrimagnets [31] or, more general, of magnetically ordered materials [38]. The fact, that the energy eigenstates of an AFM are already squeezed states and it is not necessary to squeeze them with an external drive is a distinct difference to photon squeezed states.

In Sec. II, we build upon the already given expansion of the squeezed vacuum eigenstate in the $\vec{k} = \vec{0}$ sublattice magnons [33] and extend it to include all possible wave vectors. Thereby we show that the \vec{k} -dependent probability $p_{\vec{k}}$ to find at least one pair of magnons, formed by one magnon per sublattice, with corresponding wave vector, in the squeezed vacuum is determined by the squeezing parameter $r_{\vec{k}}$. Further we found, that the number of magnons in each sublattice with antiparallel wave vector has to be the same. Therefore, they are entangled, which will be shown to be in accordance with the violation of the Duan-Giedke-Cirac-Zoller (DGCZ) inequality [39] and which is a clear hint on the quantum behaviour of magnons. In Sec. III, we show how the k -structure of $p_{\vec{k}}$ transfers to the autocorrelators of magnetization and Néel-Vector components. Finally in Sec. IV we will cope with the statistics of the sublattice magnons and

^{*} dennis.wuhrer@uni-konstanz.de

[†] niklas.rohling@uni-konstanz.de

[‡] wolfgang.belzig@uni-konstanz.de

its dependence on the system parameter $|J|/K$. All figures were made for a two-dimensional square lattice AFM with $z = 4$ next neighbours.

II. THEORETICAL MODEL

We cover a bipartite square lattice AFM with the nearest neighbours of each spin being part of the other sublattice. We do a Néel ordered ansatz along the z-axis for both sublattices. The Heisenberg interaction be on nearest neighbours only. The Hamiltonian can then be given as

$$\hat{H} = -\frac{J}{\hbar^2} \sum_{\langle i,j \rangle} \vec{S}(\vec{r}_i) \cdot \vec{S}(\vec{r}_j) - \frac{K}{\hbar^2} \sum_i \left(\hat{S}^z(\vec{r}_i) \right)^2, \quad (1)$$

with the strength of the exchange interaction $J < 0$ for AFMs, the strength of the uni-axial anisotropy along the z-axis K and $\vec{S}(\vec{r}_i)$ being the spin operator at position \vec{r}_i , with components $\hat{S}^\alpha(\vec{r}_i)$, $\alpha \in \{x, y, z\}$. The division by \hbar^2 ensures that both, J and K , have the unit of energy.

Applying the standard techniques, with the Holstein-Primakoff transformation [40] in linear approximation, the Hamiltonian becomes

$$\hat{H} = \sum_{\vec{k}} A_{\vec{k}} \left(\hat{a}_{\vec{k}}^\dagger \hat{a}_{\vec{k}} + \hat{b}_{\vec{k}}^\dagger \hat{b}_{\vec{k}} \right) + C_{\vec{k}} \left(\hat{a}_{\vec{k}}^\dagger \hat{b}_{-\vec{k}}^\dagger + \hat{a}_{\vec{k}} \hat{b}_{-\vec{k}} \right). \quad (2)$$

The different interactions are covered in the two functions, which are given as $A_{\vec{k}} = A = S(2K - Jz)$, $C_{\vec{k}} = -JSz\gamma_{\vec{k}}$ and $\gamma_{\vec{k}} = \sum_{\vec{\delta}} e^{i\vec{\delta}\vec{k}}/z$. Here, z is the number of nearest neighbours at each lattice site, which depends on the dimensionality of our system, and $\vec{\delta}$ are the connection vectors to these nearest neighbours, $\hat{a}_{\vec{k}}$ ($\hat{b}_{\vec{k}}$) is the annihilation operator of a magnon with wave vector \vec{k} in the A (B) sublattice. We set the lattice constant to $a = 1$. The diagonal components $A_{\vec{k}}$ can be \vec{k} -dependent if one does not limit to nearest-neighbour interaction. Terms arising during the manipulation of the Hamiltonian and which result in a constant energy shift are neglected.

We then perform a Bogoliubov transformation connecting the sublattice operators with new creation and annihilation operators $\hat{\alpha}$ and $\hat{\beta}$ via

$$\begin{pmatrix} \hat{a}_{\vec{k}} \\ \hat{b}_{-\vec{k}}^\dagger \end{pmatrix} = \begin{pmatrix} u_{\vec{k}} & v_{\vec{k}} \\ v_{\vec{k}}^* & u_{\vec{k}} \end{pmatrix} \begin{pmatrix} \hat{\alpha}_{\vec{k}} \\ \hat{\beta}_{-\vec{k}}^\dagger \end{pmatrix}. \quad (3)$$

The Bogoliubov transformation will diagonalize the Hamiltonian, if we demand $\hat{\alpha}$ and $\hat{\beta}$ to be bosonic operators and choose the matrix elements such, that they satisfy

$$\begin{aligned} u_{\vec{k}} &= \sqrt{\frac{A + \varepsilon_{\vec{k}}}{2\varepsilon_{\vec{k}}}}, & \varepsilon_{\vec{k}} &= \sqrt{A^2 - C_{\vec{k}}^2}, \\ v_{\vec{k}} &= -\sqrt{\frac{A - \varepsilon_{\vec{k}}}{2\varepsilon_{\vec{k}}}}, & & \end{aligned} \quad (4)$$

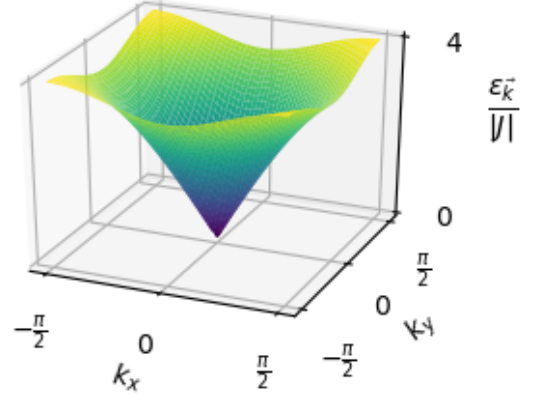


FIG. 1. Energy dispersion for a two dimensional square lattice antiferromagnet, with $|J|/K = 10^4$.

where $\varepsilon_{\vec{k}}$ is the energy of one $\hat{\alpha}$ ($\hat{\beta}$) magnon with wave vector \vec{k} .

A. Magnon squeezing

We introduce the two-mode squeezing operator [36]

$$\hat{S}_2(r_{\vec{k}}) = \exp \left[r_{\vec{k}} \left(\hat{a}_{\vec{k}} \hat{b}_{-\vec{k}} - \hat{a}_{\vec{k}}^\dagger \hat{b}_{-\vec{k}}^\dagger \right) \right], \quad (5)$$

with the positive squeezing parameter $r_{\vec{k}}$, which can be connected to the Bogoliubov transformation via $\cosh r_{\vec{k}} = u_{\vec{k}}$ and $\sinh r_{\vec{k}} = -v_{\vec{k}}$. Applying $\hat{S}_2(r_{\vec{k}})$ to the sublattice vacuum state $|0\rangle_{\text{sub}}$ creates an entangled state of both modes $\hat{a}_{\vec{k}}$ and $\hat{b}_{-\vec{k}}$. The probability $p_{\vec{k}} = \tanh^2(r_{\vec{k}}) \in [0, 1]$ to find at least one pair of magnons, build of one magnon with wave vector \vec{k} in sublattice A and one magnon with wavevector $-\vec{k}$ in sublattice B. The application of the squeezing operator results in a squeezing of the quadratures of superpositions of both modes. In the picture of two harmonic oscillators this squeezing can be imagined as a squeezing of the relative and center of mass coordinates.

The squeezing parameter determines the degree of squeezing in our system and is determined by $|J|/K$. By changing the anisotropy strength one can then tune the degree of squeezing in our system, similar to the squeezing in a ferromagnet [35].

A straightforward calculation shows, that one can write the new magnon operators as

$$\hat{\alpha}_{\vec{k}} = \hat{S}_2(r_{\vec{k}}) \hat{a}_{\vec{k}} \hat{S}_2(r_{\vec{k}})^{-1}, \quad \hat{\beta}_{\vec{k}} = \hat{S}_2(r_{\vec{k}}) \hat{b}_{\vec{k}} \hat{S}_2(r_{\vec{k}})^{-1}, \quad (6)$$

which is why we will call them "squeezed magnons" from now on.

If we denote the ground state, or vacuum state of our system as $|0\rangle_{\text{sq}}$ and the Néel state, or sublattice vacuum state, as $|0\rangle_{\text{sub}}$ and apply $\hat{\alpha}_{\vec{k}}|0\rangle_{\text{sq}} = 0$, one can show, that we can connect both vacua via [33]

$$|0\rangle_{\text{sq}} = \prod_{\vec{k}} \hat{S}_2(r_{\vec{k}}) |0\rangle_{\text{sub}}, \quad (7)$$

resulting in the squeezed vacuum being an entangled, squeezed state of sublattice modes.

By applying the squeezed annihilation operators, expressed through the Bogoliubov transformation (Eq. (3)), onto the squeezed vacuum a straightforward calculation shows

$$|0\rangle_{\text{sq}} = \sum_{\vec{n}=\vec{0}}^{\infty} \prod_{\vec{k}} \left(\frac{(-\tanh r_{\vec{k}})^{n_{\vec{k}}}}{\cosh r_{\vec{k}}} \right) |\vec{n}, \vec{m}(\vec{n})\rangle_{\text{sub}}. \quad (8)$$

Here the components of \vec{n} (\vec{m}) are the occupation numbers of the different sublattice modes in the A (B) sublattice, with $n_{\vec{k}}$ ($m_{\vec{k}}$) being the number of magnons in the mode with wave vector \vec{k} , $m_{\vec{k}}(\vec{n}) = n_{-\vec{k}}$ and

$$\begin{aligned} |\vec{n}, \vec{m}(\vec{n})\rangle_{\text{sub}} &= \bigotimes_{\vec{k}} |n_{\vec{k}}, m_{\vec{k}}(\vec{n})\rangle_{\text{sub}} = \\ &= \bigotimes_{\vec{k}} \left(|n_{\vec{k}}\rangle_{\text{sub}}^A \otimes |n_{-\vec{k}}\rangle_{\text{sub}}^B \right), \end{aligned} \quad (9)$$

where $|\dots\rangle_{\text{sub}}^{A/B}$ is a state in sublattice A (B). We see, that we only have states with the same number of magnons in the A and B sublattice for opposite wave vectors. This will guarantee us an overall vanishing momentum in each mode. Furthermore, one can show that the expectation value of the spin of a magnon in the A and a magnon in the B sublattice are antiparallel, resulting in an overall vanishing expectation value for the spin operator.

If we want a spin-up magnon of wave vector \vec{k} in the squeezed space, we have to act with a creation operator $\hat{\beta}_{\vec{k}}^{\dagger}$ onto the squeezed vacuum. Using the expression for $\hat{\beta}_{\vec{k}}^{\dagger}$ via the squeezing operator and the expansion of the squeezed vacuum, we get for the expansion of the one-magnon state

$$\begin{aligned} |\uparrow, \vec{k}\rangle_{\text{sq}} &= \sum_{\vec{n}=\vec{0}}^{\infty} \left[\prod_{\vec{k}' \neq \vec{k}} \left(\frac{(-\tanh r_{\vec{k}'})^{n_{\vec{k}'}}}{\cosh r_{\vec{k}'}} \right) \right. \\ &\quad \left. \times \frac{\sqrt{n_{\vec{k}} + 1} (-\tanh r_{\vec{k}})^{n_{\vec{k}}}}{\cosh^2 r_{\vec{k}}} |\vec{n}, \vec{m}(\vec{n}) + \vec{e}_{\vec{k}}\rangle_{\text{sub}} \right]. \end{aligned} \quad (10)$$

In contrast to the squeezed vacuum state, we can see, that only sublattice states contribute, if they contain one magnon with wave vector \vec{k} more in the B sublattice, than magnons with wave vector $-\vec{k}$ in the A sublattice. The only probability amplitude, which is changed in the

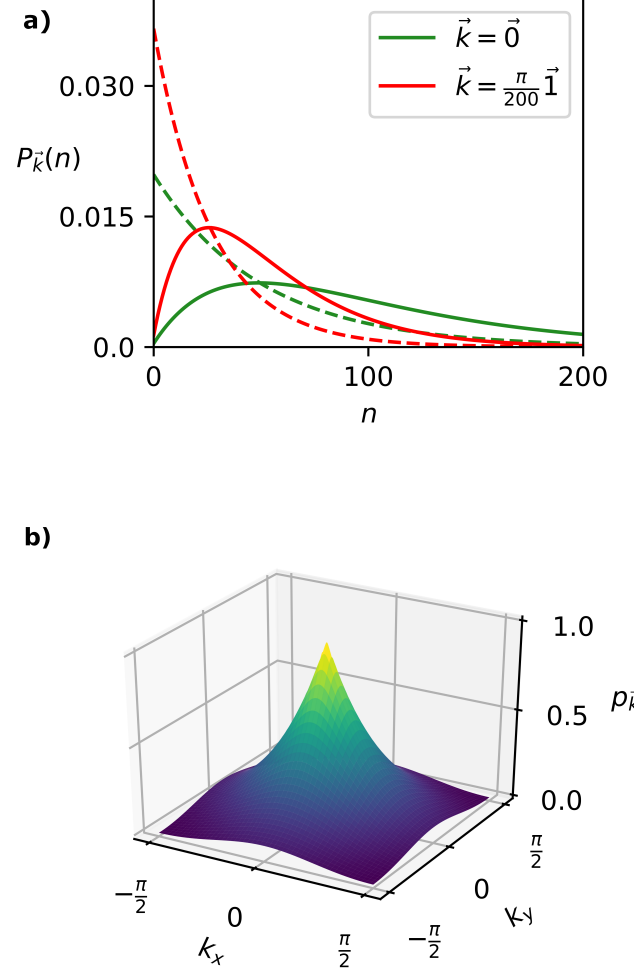


FIG. 2. Both figures were made for $|J|/K = 10^4$. a) Probability $P_{\vec{k}}(n)$ to find n magnons in sublattice A/B with wave vector $\vec{k} = \vec{0}$ (green) and $\vec{k} = \frac{\pi}{200} \vec{1}$ (red) in the squeezed vacuum state (dashed) and the probability $Q_{\vec{k}}(n)$ to find n magnons in sublattice A/B and $n+1$ in B/A in the squeezed magnon state (solid). Here $\vec{1} = (1, 1)^T$. b) Probability $p_{\vec{k}}$ to have at least one magnon in each sublattice. We see a sharp peak at $\vec{k} = \vec{0}$, with $p_{\vec{0}} \approx 0.6$, implying, that the probability to find any number of magnons different from 0 for the other wave vectors is very small.

squeezed magnon state with wave vector \vec{k} , is the probability amplitude for the \vec{k} sublattice modes.

Applying $\hat{\alpha}_{\vec{k}}^{\dagger}$ onto the squeezed vacuum would lead to a squeezed spin down magnon with the same probability amplitudes for the sublattice states, but we would get one magnon with wave vector \vec{k} more in the A sublattice than $-\vec{k}$ magnons in the B sublattice. In Eq. (8) and Eq. (10) we can see that the probability amplitude and therefore the probability takes the same form for all wave vectors, only differing through $r_{\vec{k}}$.

For the squeezed vacuum the probability to find n pairs

of magnons, consisting of one magnon in sublattice A with wave vector \vec{k} and one magnon in sublattice B with wave vector $-\vec{k}$, can be given as

$$P_{\vec{k}}(n) = \frac{\tanh(r_{\vec{k}})^{2n}}{\cosh(r_{\vec{k}})^2} = (1 - p_{\vec{k}}) p_{\vec{k}}^n. \quad (11)$$

The probability for a squeezed spin up (down) magnon with wave vector \vec{k} containing $n + 1$ sublattice magnons of wave vector \vec{k} in sublattice B (A) and n sublattice magnons of wave vector $-\vec{k}$ in sublattice A (B) can also be expressed through $p_{\vec{k}}$ by

$$Q_{\vec{k}}(n) = (1 - p_{\vec{k}})^2 (n + 1) p_{\vec{k}}^n. \quad (12)$$

Figure 2a) shows the dependence of $P_{\vec{k}}(n)$ and $Q_{\vec{k}}(n)$ on n for the two wave vectors $\vec{k} = \vec{0}$ and $\vec{k} = \frac{\pi}{200}(1, 1)^\top$. While in the vacuum state each $P_{\vec{k}}(n)$ falls off exponentially with the maximum at $n = 0$, this changes for $Q_{\vec{k}}(n)$, in the case of a squeezed magnon, where the function is nonmonotonic, with a maximum at some n different from zero. This behaviour is similar for all \vec{k} , but the closer to the edge of the Brillouin zone \vec{k} is, the steeper the probability falls off around $n = 0$ for the vacuum state and the closer is the maximum of $Q_{\vec{k}}(n)$ to zero. This behaviour can be seen in Fig. 2b), which shows $p_{\vec{k}}$, i.e. the probability to find at least one pair of magnons in the sublattices with corresponding wave vectors. As $p_{\vec{k}}$ goes towards zero for large wave vectors the expectation value should be centered more around zero magnons, which is confirmed by Fig. 2a).

B. DGCZ inequality

From the full expansion of the squeezed vacuum and one-magnon state we can see, that we cannot separate the $\hat{a}_{\vec{k}}$ and $\hat{b}_{-\vec{k}}$ modes resulting in an entanglement of both modes. This entanglement is confirmed by the DGCZ inequality [39], which states, that for any separable quantum state the total variance of a pair of operators

$$\begin{aligned} \hat{u} &= |c| \hat{x}_1 + \frac{1}{c} \hat{x}_2, & [\hat{x}_i, \hat{p}_j] &= i\delta_{i,j}, \\ \hat{v} &= |c| \hat{p}_1 - \frac{1}{c} \hat{p}_2, & c &\in \mathbb{R} \setminus \{0\} \end{aligned} \quad (13)$$

satisfies the inequality

$$\langle (\Delta \hat{u})^2 \rangle + \langle (\Delta \hat{v})^2 \rangle \geq c^2 + \frac{1}{c^2}. \quad (14)$$

If we use the sublattice annihilation and creation operators to define

$$\begin{aligned} \hat{x}_1 &= \frac{1}{\sqrt{2}} (\hat{a}_{\vec{k}} + \hat{a}_{\vec{k}}^\dagger), & \hat{p}_1 &= \frac{1}{\sqrt{2i}} (\hat{a}_{\vec{k}} - \hat{a}_{\vec{k}}^\dagger), \\ \hat{x}_2 &= \frac{1}{\sqrt{2}} (\hat{b}_{\vec{k}'} + \hat{b}_{\vec{k}'}^\dagger), & \hat{p}_2 &= \frac{1}{\sqrt{2i}} (\hat{b}_{\vec{k}'} - \hat{b}_{\vec{k}'}^\dagger), \end{aligned} \quad (15)$$

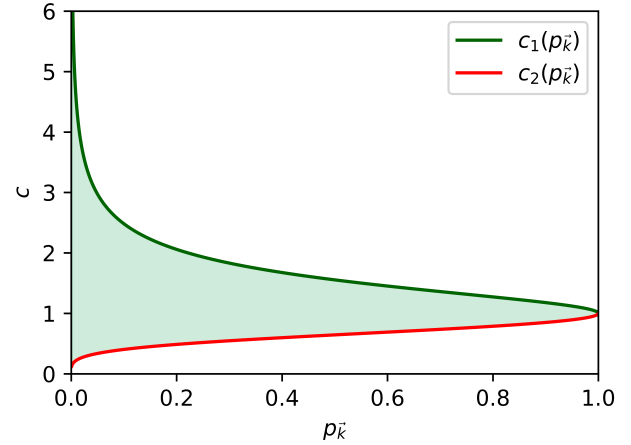


FIG. 3. Values for c , depending on $p_{\vec{k}}$, which violate the DGCZ inequality (green area). The green (red) line satisfies the equality and correspond to solution c_1 (c_2).

then $[\hat{x}_i, \hat{p}_j] = i\delta_{i,j}$ is obviously fulfilled. If we regard the squeezed vacuum state, indicated through the subscript 'sq' further on, we can show for $\vec{k}' \neq -\vec{k}$

$$\begin{aligned} \langle (\Delta \hat{u})^2 \rangle_{\text{sq}} + \langle (\Delta \hat{v})^2 \rangle_{\text{sq}} &= c^2 \frac{1 + p_{\vec{k}}}{1 - p_{\vec{k}}} + \frac{1}{c^2} \frac{1 + p_{\vec{k}'}}{1 - p_{\vec{k}'}} \\ &\geq c^2 + \frac{1}{c^2} \end{aligned} \quad (16)$$

the inequality is always fulfilled. For modes $\vec{k}' = -\vec{k}$ we get

$$\begin{aligned} \langle (\Delta \hat{u})^2 \rangle_{\text{sq}} + \langle (\Delta \hat{v})^2 \rangle_{\text{sq}} &= \left(c^2 + \frac{1}{c^2} \right) \frac{1 + p_{\vec{k}}}{1 - p_{\vec{k}}} \\ &\quad - 4 \frac{|c|}{c} \frac{\sqrt{p_{\vec{k}}}}{1 - p_{\vec{k}}}. \end{aligned} \quad (17)$$

If we use this equation and demand the DGCZ inequality to be an equality, we can solve this for c ,

$$c_{1/2} = \sqrt{\frac{1}{\sqrt{p_{\vec{k}}}} (1 \pm \sqrt{1 - p_{\vec{k}}})}. \quad (18)$$

Due to the absolute value of c , which plays a role in the DGCZ equation, only the positive solutions $c_{1/2}$ solve the problem at hand. All values for c enclosed by these both branches, which we can see in Fig. 3, violate the inequality. From this follows, that all modes $\hat{a}_{\vec{k}}$ and $\hat{b}_{-\vec{k}}$ are entangled, which supports our earlier claim.

III. CORRELATORS

The k -space structure of $p_{\vec{k}}$ transfers to the k -space structure of the autocorrelators of the magnetization and

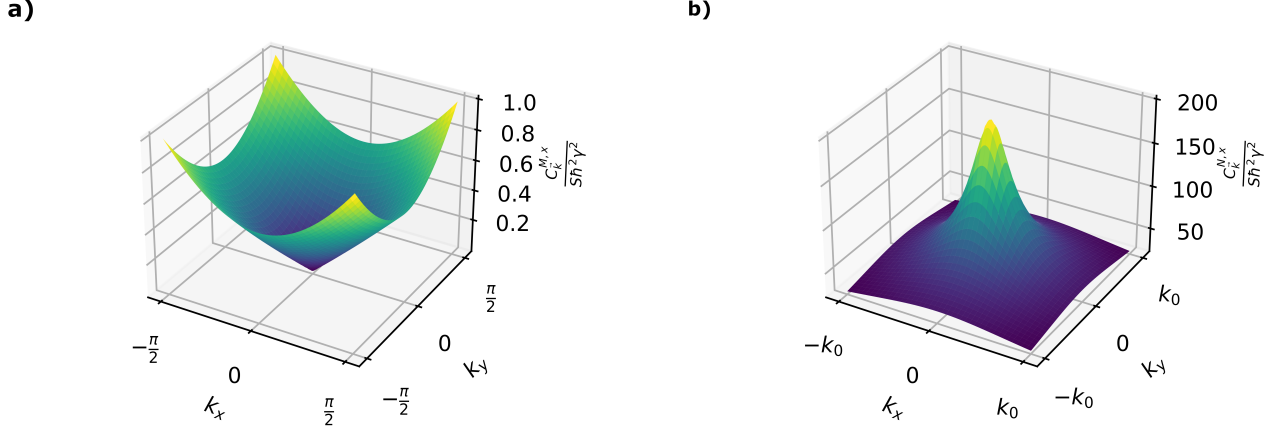


FIG. 4. Autocorrelator of the x-components of the magnetization (left) and Néel vector (right) in the k space for $|J|/K = 10^4$. The k_x and k_y values are limited to $k_0 = 0.076$ in picture b) to keep the focus on points with $C_k^{N,x} > 1$. For the value of k_0 see App. B.

Néel vector components, which includes the uncertainty of each variable. The magnetization of an AFM is defined as the sum of the sublattice magnetizations, while the Néel vector is the difference of them. At a point \vec{r} at the lattice both of them are defined as

$$\vec{M}(\vec{r}) = \gamma \begin{cases} \vec{S}^A(\vec{r}) & \vec{r} \in A \\ \vec{S}^B(\vec{r}) & \vec{r} \in B \end{cases}, \quad (19)$$

$$\vec{N}(\vec{r}) = \gamma \begin{cases} \vec{S}^A(\vec{r}) & \vec{r} \in A \\ -\vec{S}^B(\vec{r}) & \vec{r} \in B \end{cases}. \quad (20)$$

Here γ is the gyromagnetic ratio. In \vec{k} -space they are given by

$$\vec{M}_{\vec{k}} = \gamma \left(\vec{S}_{\vec{k}}^A + \vec{S}_{\vec{k}}^B \right), \quad \vec{N}_{\vec{k}} = \gamma \left(\vec{S}_{\vec{k}}^A - \vec{S}_{\vec{k}}^B \right). \quad (21)$$

As before $\vec{S}_{\vec{k}}^A$ is connected to the sublattice creation and annihilation operators via the linearised Holstein-Primakoff transformation. This connection yields for the x,y-components of the magnetization and the Néel vector in terms of creation and annihilation operators

$$M_{\vec{k}}^x = \gamma \hbar \frac{\sqrt{2S}}{2} \left(\hat{a}_{\vec{k}} + \hat{a}_{-\vec{k}}^\dagger + \hat{b}_{\vec{k}} + \hat{b}_{-\vec{k}}^\dagger \right), \quad (22)$$

$$M_{\vec{k}}^y = \gamma \hbar \frac{\sqrt{2S}}{2i} \left(\hat{a}_{\vec{k}} - \hat{a}_{-\vec{k}}^\dagger - \hat{b}_{\vec{k}} + \hat{b}_{-\vec{k}}^\dagger \right), \quad (23)$$

$$N_{\vec{k}}^x = \gamma \hbar \frac{\sqrt{2S}}{2} \left(\hat{a}_{\vec{k}} + \hat{a}_{-\vec{k}}^\dagger - \hat{b}_{\vec{k}} - \hat{b}_{-\vec{k}}^\dagger \right), \quad (24)$$

$$N_{\vec{k}}^y = \gamma \hbar \frac{\sqrt{2S}}{2i} \left(\hat{a}_{\vec{k}} - \hat{a}_{-\vec{k}}^\dagger + \hat{b}_{\vec{k}} - \hat{b}_{-\vec{k}}^\dagger \right). \quad (25)$$

The correlator of two operators \vec{A} and \vec{B} with components \hat{A}^α and \hat{B}^β ($\alpha, \beta \in \{x, y, z, +, -\}$) at point \vec{k} in the k -space space is defined as

$$C_{\vec{k}}^{A,B|\alpha,\beta} = \left\langle \hat{A}_{\vec{k}}^\alpha \hat{B}_{\vec{k}}^{\beta\dagger} \right\rangle - \left\langle \hat{A}_{\vec{k}}^\alpha \right\rangle \left\langle \hat{B}_{\vec{k}}^{\beta\dagger} \right\rangle \quad (26)$$

Due to translation symmetry, same \vec{k} values in both operators are the only points in the k -space at which the correlators for magnetization and Néel vector components will be non-zero. Keeping in Mind, that $\hat{M}_{\vec{k}}^{x\dagger} = \hat{M}_{-\vec{k}}^x$ and similar for other components and the Néel vector, the autocorrelators becomes

$$C_{\vec{k}}^{M,x} = C_{\vec{k}}^{M,y} = S \hbar^2 \gamma^2 \frac{1 - \sqrt{p_{\vec{k}}}}{1 + \sqrt{p_{\vec{k}}}} = S \hbar^2 \gamma^2 e^{-2|r_{\vec{k}}|}, \quad (27)$$

$$C_{\vec{k}}^{N,x} = C_{\vec{k}}^{N,y} = S \hbar^2 \gamma^2 \frac{1 + \sqrt{p_{\vec{k}}}}{1 - \sqrt{p_{\vec{k}}}} = S \hbar^2 \gamma^2 e^{+2|r_{\vec{k}}|}. \quad (28)$$

The dependence of the autocorrelators on the wave vector components k_x and k_y can be seen in Fig. 4. The strongest correlation for the magnetization is at the edge of the Brillouin zone and the weakest at the center $\vec{k} = 0$, which is the opposite as in the case of the Néel vector. For the Néel vector the strongest correlations lie in a circle with radius $k_0 = \sqrt{2K/|J|}$ around the origin. This value for $|\vec{k}|$ determines the point at which the energy dispersion relation can be assumed to be linear, as shown in B.

Using the results from section II one can connect them to the autocorrelators by choosing $c = \pm 1$, $\vec{k}' = -\vec{k}$ and multiplying \hat{x}_i and \hat{p}_i with $\sqrt{2S}\hbar\gamma$ in Eq. 13, which results in

$$\left\langle (\Delta\hat{u})^2 \right\rangle_{\text{sq}} + \left\langle (\Delta\hat{v})^2 \right\rangle_{\text{sq}} = \begin{cases} 4 \left\langle M_{\vec{k}}^x M_{\vec{k}}^{x\dagger} \right\rangle_{\text{sq}} & (+) \\ 4 \left\langle N_{\vec{k}}^y N_{\vec{k}}^{y\dagger} \right\rangle_{\text{sq}} & (-), \end{cases} \quad (29)$$

where we used $C_{\vec{k}}^{N/M,x} = C_{\vec{k}}^{N/M,y}$ (Eq. (27)+(28)). This is in accordance with the choice of c and the earlier calculated violation of the inequality. This means, for

$c = 1$ the inequality is always violated, resulting in $\langle M_k^x M_k^{x\dagger} \rangle_{\text{sq}} \leq S\hbar^2\gamma^2$, as can be seen from Eq. (27). For $c = -1$ the inequality is always fulfilled, resulting in $\langle N_k^y N_k^{y\dagger} \rangle_{\text{sq}} \geq S\hbar^2\gamma^2$, as can be seen from Eq. (28). From these inequalities we can see, that the squeezing property of the squeezed vacuum results in a squeezing of the magnetization and Néel vector autocorrelators. While one becomes smaller, the other becomes bigger, but the product of both of stays always the same

$$\langle M_k^x M_k^{x\dagger} \rangle_{\text{sq}} \langle N_k^y N_k^{y\dagger} \rangle_{\text{sq}} = (S\hbar^2\gamma^2)^2. \quad (30)$$

It is important to note here, that the product of the uncertainty of the same spatial components of the Néel vector and the magnetization results also in $(S\hbar^2\gamma^2)^2$. While the above relation seems to indicate a squeezing between, for example, for M_k^x and N_k^x , we want to emphasize, that $[M_k^\alpha, N_{-k}^\beta] = 2iS\hbar^2\gamma^2(1 - \delta_{\alpha,\beta})$, $\alpha, \beta \in \{x, y\}$. Regarding the uncertainty principle [41], the commutator yields, that while for different spatial components the uncertainty is minimal, this is not true for the same spatial components.

For the correlators in z-direction, if we only regard the terms up to order two in the creation and annihilation operators, then the autocorrelators vanish. The cross-correlators for different components of the same vectors, e.g. $C_{\vec{k}}^{M|x,y}$ or $C_{\vec{k}}^{M|z,x}$, also vanish, as well as the cross-correlators of the same component of different vectors.

The only other, non-vanishing crosscorrelator is between the x - and y -components of the magnetization and the Néel vector, which is given as

$$C_{\vec{k}}^{M,N|x,y} = i\gamma^2 S\hbar^2. \quad (31)$$

This is a purely imaginary result. However, an expectation value of a measurable quantity must be real. We want to note, that such a measurable quantity is expressed by the anticommutator of M_k^x and N_k^y , which is a Hermitian operator and therefore results in a real expectation value, which is equal to 0.

The final result of this section is the relation between the autocorrelators of the magnetization modes and the Néel vector modes. It always holds

$$C_{\vec{k}}^{M,x} \leq C_{\vec{k}}^{N,y}. \quad (32)$$

The relation between the correlators is of utmost importance as measurement and comparison of the different correlators can be used to determine a clear experimental signature of a squeezed magnonic ground state.

IV. MAGNON NUMBER

Finally, we want to investigate the number of magnons per sublattice in the squeezed vacuum of our system.

Therefore, we calculate the expectation value and variance of $\hat{n} = \sum_{\vec{k}} \hat{a}_{\vec{k}}^\dagger \hat{a}_{\vec{k}}$, which is the number operator of all sublattice magnons of sublattice A. The number of magnons in sublattice B is equal in the squeezed vacuum. We use the expansion of the squeezed vacuum in sublattice states in Eq. (8) and obtain the expectation value

$$\langle \hat{n} \rangle_{\text{sq}} = \sum_{\vec{k}} \frac{p_{\vec{k}}}{1 - p_{\vec{k}}} = \sum_{\vec{k}} \sinh^2(r_{\vec{k}}) \quad (33)$$

and the variance

$$\begin{aligned} \langle (\Delta \hat{n})^2 \rangle_{\text{sq}} &= \sum_{\vec{k}} \langle \hat{n}_{\vec{k}} \rangle_{\text{sq}} \left(\langle \hat{n}_{\vec{k}} \rangle_{\text{sq}} + 1 \right) = \\ &= \sum_{\vec{k}} \frac{p_{\vec{k}}}{(1 - p_{\vec{k}})^2} = \sum_{\vec{k}} \cosh^2(r_{\vec{k}}) \sinh^2(r_{\vec{k}}). \end{aligned} \quad (34)$$

We can see from Eq. (33) that with rising number of possible magnon modes, i.e. with increasing system size, the expectation value as well as the variance will rise. This shows that these are extensive quantities as one would expect it for the number of particles.

To compare systems of different sizes we will divide these quantities by the number of modes N , i.e. the number of possible \vec{k} values, with $\tilde{n} = \hat{n}/N$. The expectation value $\langle \tilde{n} \rangle$ can then be seen as the average occupation number and the variance $\langle (\Delta \hat{n})^2 \rangle / N$ as average variance per mode. Our system is fully characterized by the ratio $|J|/K$. This characterization can be seen from Eq. (4), as it connects $p_{\vec{k}}$, and therefore the other quantities, with $|J|/K$. Therefore, if we decide on a certain type of lattice, the ratio of $|J|$ and K determines the number of sublattice magnons which are involved in the building of the squeezed states.

Fig. 5 shows the dependence of $\langle \tilde{n} \rangle$ and $\langle (\Delta \hat{n})^2 \rangle / N$ on $|J|/K$ in a double logarithmic plot with basis 10. The different graphs are given for distinct system sizes, i.e. distinct N . Nevertheless, one can see a few common features, e.g. the overall form of $\langle \tilde{n} \rangle$ with a saturation around $\langle \tilde{n} \rangle \approx 0.35$. As this can be interpreted as the average occupation number of the different modes, we can assume the linear approximation of the Holstein-Primakoff transformation, which demands a small number of magnons per mode, to hold. Only in the case of small samples one gets a strong deviation implying, that in this case we should consider higher terms in the creation and annihilation operators. This is reasonable, as we expect finite size effects to become important in such a case.

The dashed line in Fig. 5 a) gives an approximation of the $|J|/K$ value beyond which the plateau and a linear behaviour starts for the 10×10 sublattice. Theoretically this point can be given for all sizes but is shifted far to the right in the case of bigger samples. It can be derived by regarding the large $|J|/K$ limit of the expectation value

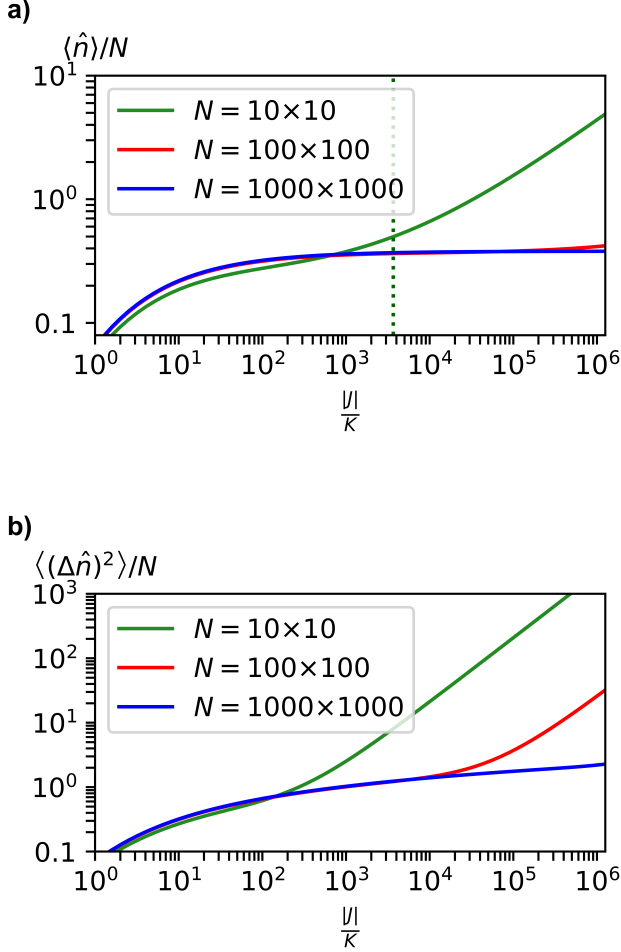


FIG. 5. Double logarithmic plot of $\langle \hat{n} \rangle$ (Fig. a) and $\langle (\Delta \hat{n})^2 \rangle_{\text{sq}} / N$ (Fig. b) depending on $|J|/K$. The number of total modes varies from graph to graph indicated by the number of lattice sites per sublattice N . The vertical, dotted line in a) shows the value for $|J|/K$, at which the $\vec{k} = \vec{0}$ contribution to the total magnon number is as big as the total contribution from all other modes. This indicates the start of the linear behaviour for the magnon number in the double logarithmic plot.

of the magnon numbers for different \vec{k} values

$$\langle \hat{n}_{\vec{k}} \rangle \Big|_{\frac{|J|}{K} \gg 1} \begin{cases} \frac{1}{2} \sqrt{\frac{|J|}{K}} & |\vec{k}| \leq \sqrt{\frac{2K}{|J|}} \\ \frac{1}{2\sqrt{1-\gamma_{\vec{k}}^2}} - \frac{1}{2} & |\vec{k}| \geq \sqrt{\frac{2K}{|J|}} \end{cases} \quad (35)$$

The square root dependency comes from the modes with $|\vec{k}| \leq \sqrt{K/(2|J|)}$, which goes towards the sole mode of $\vec{k} = \vec{0}$ for $|J|/K \rightarrow \infty$. This is the same point at which a linear dependence of the energy on the absolute value of the wave vector is to be expected, as the contribution of the wave vector dependent part begins to dominate the

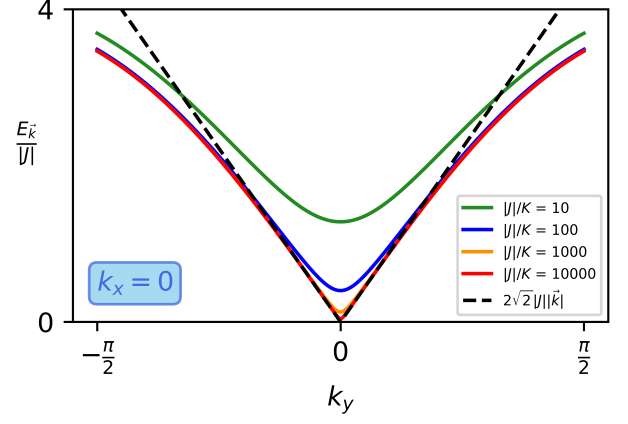


FIG. 6. Ratio of energy and $|J|$ for different values of $|J|/K$ and $J = -1$ showing the lowering of the energy gap for smaller K and the approach to a linear dispersion. Dashed black line gives the linear dispersion with $\varepsilon_{\vec{k}}/|J| = 2\sqrt{2}|\vec{k}|$.

energy. See therefore App. B.

For modes with $|\vec{k}|$ bigger than this value the contribution saturates at a , with respect to $|J|/K$, constant value. An approximation of the point the linear behaviour in the double logarithmic plot starts is given, when the $\frac{1}{2}\sqrt{|J|/K}$ contribution of the $|\vec{k}| \leq \sqrt{K/(2|J|)}$ modes overcomes the contribution of the other modes in this limit.

From Eq. (34) it can be seen, that the variance, if plotted double logarithmically, also starts to grow linearly in $|J|/K$ for large values. The slope will be two times as big as for the expectation value. This implies, that even if the expectation value of the average occupation number grows, the variance of values the occupation numbers of different modes can take grows even faster.

The divergence of the magnon number, arises, because the energy gap Δ goes towards zero for $K \rightarrow 0$, finally becoming zero for $K = 0$ (see Fig. 6). Therefore, as magnons are bosons, an infinite number of magnons would be created, which populate the lowest energy level ($\vec{k} = \vec{0}$). As the infinite number of sublattice magnons indicates, our theory does fail in this regime, as the approximation of small occupation numbers made in the Holstein-Primakoff transformation does not hold any more.

On the other side, if K becomes very large, i.e. $|J|/K \rightarrow 0$, we get vanishing expectation value. This is obviously due to the fact, that the energy gap becomes arbitrary large. In the model of moving spins this can be imagined as spins fixed in their position through the arbitrarily strong anisotropy and being unable to move, which makes it impossible for magnons, as they are collective spin excitations, to exist.

The number of sublattice magnon building the differ-

ent squeezed eigenstates of the system are of special interest due to their influence on interactions applied to the system. If the interaction couples to the eigenmodes of the system, which means to the squeezed magnons, it would be small, in the one magnon case, or zero in the vacuum case. But if the interaction couples to the number of sublattice magnons the influence would be huge even in the vacuum state. The interaction strength should then depend on the system size and $|J|/K$.

V. CONCLUSION

We picked up the work from Kamra et al. [33] and further included all possible sublattice magnon states into the expansion of the squeezed magnon states. We were able to show that the probability amplitude takes the same form for each component only differing by the squeezing factor $r_{\vec{k}}$.

From the squeezing parameter we determined the k -space structure of the probability to find at least one pair of sublattice magnons, formed by one magnon in sublattice A with wave vector \vec{k} and one magnon in sublattice B with wave vector $-\vec{k}$, which resulted in a k -space structure of the autocorrelators of the magnetization and the Néel vector components. This gives us experimental access to the probability structure by measurement and comparison of these correlators. Further we also determined the crosscorrelators between the x -component of the magnetization and the y -component of the Néel vector, which is purely imaginary and vanishes if we regard a symmetrized version, by using the anticommutator of the x -component of the magnetization and the y -component of the Néel vector.

We determined the expectation value and variance of the occupation number of each magnon mode each sublattice and from this we obtained the $|J|/K$ dependence of the average occupation number of magnons in the system. We found that the average occupation number behaves similarly for different system sizes. From the expectation value of the number of sublattice magnons it is possible to identify the strength of the influence of different interactions on our Heisenberg AFM by their coupling either to sublattice magnons or squeezed magnons.

Further investigations could concentrate on the effect of an applied magnetic field on the number of sublattice magnons participating in the squeezed Fock state. For a static magnetic field we expect a change in the number of $\vec{k} = \vec{0}$ magnons, which will result in a simultaneous tilt of all sublattice spins.

Post completion note: After finishing this work, but before publishing, the authors became aware of the recent publication of Mousolou et. al.[42], which has a certain overlap with topics discussed above. While there are common themes, like the parameterization of relevant quantities in terms of the squeezing parameter $r_{\vec{k}}$, there are also differences, as the main focus on the entanglement entropy and a suggestion for an experimental

setup in Mousolou et. al. work, while our publication is focused on the correlators of the magnetization and the Néel vector as well as the occupation number of magnons and their variance. We therefore see both works as complementary to each other.

ACKNOWLEDGMENT

We acknowledge useful discussions with Akashdeep Kamra. This work was financially supported by the Deutsche Forschungsgemeinschaft (DFG, German Research Foundation) via the Collaborative Research Center SFB 1432 (project no. 425217212) and via the Priority Program SPP 2244 (project no. 443404566). NR acknowledges financial support by the DFG via the project no. 417034116.

Appendix A: Expansion of squeezed states in sublattice states

We start the expansion of the squeezed vacuum state in the sublattice states by acting with $\hat{\alpha}_{\vec{k}}$ onto the squeezed vacuum state and use the Bogoliubov transformation to determine the expansion coefficients

$$\hat{\alpha}_{\vec{k}} |0\rangle_{\text{sq}} = \sum_{\vec{n}, \vec{m}=0}^{\infty} A_{\vec{n}, \vec{m}} \left(u_{\vec{k}} \hat{a}_{\vec{k}} - v_{\vec{k}} \hat{b}_{-\vec{k}}^{\dagger} \right) |\vec{n}, \vec{m}\rangle_{\text{sub}} = 0. \quad (\text{A1})$$

Here \vec{n} (\vec{m}) contains the number of sublattice magnons with certain wave vectors in the A (B) sublattice. Doing the same with $\hat{\beta}_{\vec{k}}$ results in the following two equations

$$A_{\vec{n}, \vec{m}} = -\tanh(r_{\vec{k}}) \sqrt{\frac{m_{-\vec{k}}}{n_{\vec{k}}}} A_{\vec{n}-\vec{e}_{\vec{k}}, \vec{m}-\vec{e}_{-\vec{k}}}, \quad (\text{A2})$$

$$A_{\vec{n}, \vec{m}} = -\tanh(r_{\vec{k}}) \sqrt{\frac{n_{-\vec{k}}}{m_{\vec{k}}}} A_{\vec{n}-\vec{e}_{-\vec{k}}, \vec{m}-\vec{e}_{\vec{k}}}. \quad (\text{A3})$$

These two equations yield, that the number of magnon with opposite wave vector in each sublattice is the same and a recursion relation, which lets us determine the factors $A_{\vec{n}, \vec{m}}$ in terms of the lowest coefficient $A_{0,0}$. $A_{0,0}$ can then be determined by the normalization condition of the squeezed vacuum. This all together yields

$$A_{\vec{n}, \vec{m}} = A_{\vec{n}} = \prod_{\vec{k}} \left[\frac{(-\tanh(r_{\vec{k}}))^{n_{\vec{k}}}}{\cosh(r_{\vec{k}})} \right]. \quad (\text{A4})$$

Appendix B: Linearity of the energy dispersion relation

For Fig. 4 b) we limited the wave vector components on a value k_0 . In Eq. (35) we reverted to a value for

the absolute value of \vec{k} for the conditional occupation number. Both values are the same and stem from the following analysis. If one assumes small values for the wave vector, one can approximate

$$\sum_{\alpha} \cos(k_{\alpha}) \approx N - \frac{\vec{k}^2}{2} \quad \alpha \in \{x_1, \dots, x_N\}. \quad (\text{B1})$$

Regarding a square lattice with nearest neighbour interaction only we know that the dimension is half the number of nearest neighbours z . In the energy dispersion relation (Eq. (4)) this yields

$$\varepsilon_{\vec{k}} = \sqrt{A^2 - C_0^2 \left(1 - \frac{2\vec{k}^2}{z}\right)}. \quad (\text{B2})$$

We now determine the value for $|\vec{k}_0|$, by demanding, that the term proportional to \vec{k}^2 is as large as the other terms. This yields

$$|\vec{k}_0| = \sqrt{\frac{z}{2} \frac{A^2 - C_0^2}{C_0^2}} = \sqrt{\frac{z}{2} \frac{(1 - \frac{Jz}{2K})}{(\frac{Jz}{2K})^2}} \quad (\text{B3})$$

$$\stackrel{|J|/K \gg 1}{\approx} \sqrt{\frac{2K}{|J|}}. \quad (\text{B4})$$

For wave vectors around this point we get a linear dispersion relation for the energy, as we can approximate

$$\begin{aligned} \varepsilon_{\vec{k}} &\approx \sqrt{2(A^2 - C_0^2)} + \sqrt{\frac{2}{z} C_0^2} \left(|\vec{k}| - |\vec{k}_0| \right) \\ &= \sqrt{A^2 - C_0^2} + \sqrt{\frac{2}{z} C_0^2} |\vec{k}|. \end{aligned} \quad (\text{B5})$$

Appendix C: Correlators

We want to give a short derivation of the correlators. starting from Eq. (21) we define

$$\vec{S}_{\vec{k}} = \vec{S}_{\vec{k}}^A + \vec{S}_{\vec{k}}^B, \quad \vec{Q} = \vec{S}_{\vec{k}}^A - \vec{S}_{\vec{k}}^B. \quad (\text{C1})$$

The magnetization (Néel vector) is then given as $\vec{M}_{\vec{k}} = \gamma \vec{S}_{\vec{k}}$ ($\vec{N}_{\vec{k}} = \gamma \vec{Q}_{\vec{k}}$).

a. x - y -Components

We are interested in the correlators of the ladder components $\hat{S}_{\vec{k}}^{\pm}$ and $\hat{Q}_{\vec{k}}^{\pm}$ as they determine the correlators of the x and y components. Due to the definition of the Fourier components of the ladder operators we get

$$\begin{aligned} \hat{S}_{\vec{k}}^{A,+} &= \sqrt{\frac{2}{N}} \sum_{\vec{r} \in A} e^{i\vec{k}\vec{r}} \sqrt{2S\hbar^2} \hat{a}(\vec{r}) = \sqrt{2S\hbar^2} \hat{a}_{\vec{k}}, \\ \hat{S}_{\vec{k}}^{A,-} &= \sqrt{\frac{2}{N}} \sum_{\vec{r} \in A} e^{i\vec{k}\vec{r}} \sqrt{2S\hbar^2} \hat{a}^{\dagger}(\vec{r}) = \sqrt{2S\hbar^2} \hat{a}_{-\vec{k}}^{\dagger}, \end{aligned} \quad (\text{C2})$$

with a similar expression for the B sublattice. Here N is the number of sites in the system. The factor $N/2$ in the transformation stems from the fact, that we have two sublattices and regard the waves on each of them. We get for $\hat{S}_{\vec{k}}^{\pm}$

$$\begin{aligned} \hat{S}_{\vec{k}}^+ &= S_{\vec{k}}^{A,+} + S_{\vec{k}}^{B,+} = \sqrt{2S\hbar^2} \left(\hat{a}_{\vec{k}} + \hat{b}_{-\vec{k}}^{\dagger} \right) = \\ &= \hbar\sqrt{2S} \left[\left(u_{\vec{k}} + v_{\vec{k}}^* \right) \hat{\alpha}_{\vec{k}} + \left(u_{\vec{k}} + v_{\vec{k}} \right) \hat{\beta}_{-\vec{k}}^{\dagger} \right] \\ &= \left(\hat{S}_{-\vec{k}}^- \right)^{\dagger}, \end{aligned} \quad (\text{C3})$$

$$\begin{aligned} \hat{Q}_{\vec{k}}^+ &= S_{\vec{k}}^{A,+} - S_{\vec{k}}^{B,+} = \sqrt{2S\hbar^2} \left(\hat{a}_{\vec{k}} - \hat{b}_{-\vec{k}}^{\dagger} \right) = \\ &= \hbar\sqrt{2S} \left[\left(u_{\vec{k}} - v_{\vec{k}}^* \right) \hat{\alpha}_{\vec{k}} - \left(u_{\vec{k}} - v_{\vec{k}} \right) \hat{\beta}_{-\vec{k}}^{\dagger} \right] \\ &= \left(\hat{Q}_{-\vec{k}}^- \right)^{\dagger}. \end{aligned} \quad (\text{C4})$$

Now one calculates the different combinations of products, i.e. $++$, $+-$, $-+$ and $--$, and takes the expectation value with respect to the squeezed vacuum. Only terms which contain the same number of creation and annihilation operators of the same kind of magnons can contribute. Further, as we are in the vacuum of the squeezed magnon modes, only modes with all creation operators on the right and all annihilation operator on the left are non-zero. This reduces the expectation values to

$$\begin{aligned} \left\langle \hat{S}_{\vec{k}}^+ \hat{S}_{\vec{q}}^- \right\rangle_{\text{sq}} &= 2S\hbar^2 \left(u_{\vec{k}} + v_{\vec{k}}^* \right) \left(u_{\vec{q}} + v_{\vec{q}} \right) \left\langle \hat{\alpha}_{\vec{k}} \hat{\alpha}_{-\vec{q}}^{\dagger} \right\rangle_{\text{sq}} = \\ &= 2S\hbar^2 \left| u_{\vec{k}} + v_{\vec{k}}^* \right|^2 \delta_{\vec{k}, -\vec{q}}, \end{aligned} \quad (\text{C5})$$

$$\begin{aligned} \left\langle \hat{Q}_{\vec{k}}^+ \hat{Q}_{\vec{q}}^- \right\rangle_{\text{sq}} &= 2S\hbar^2 \left(u_{\vec{k}} - v_{\vec{k}}^* \right) \left(u_{\vec{q}} - v_{\vec{q}} \right) \left\langle \hat{\alpha}_{\vec{k}} \hat{\alpha}_{-\vec{q}}^{\dagger} \right\rangle_{\text{sq}} = \\ &= 2S\hbar^2 \left| u_{\vec{k}} - v_{\vec{k}}^* \right|^2 \delta_{\vec{k}, -\vec{q}}, \end{aligned} \quad (\text{C6})$$

$$\begin{aligned} \left\langle \hat{S}_{\vec{k}}^+ \hat{Q}_{\vec{q}}^- \right\rangle_{\text{sq}} &= 2S\hbar^2 \left(u_{\vec{k}} + v_{\vec{k}}^* \right) \left(u_{\vec{q}} - v_{\vec{q}} \right) \left\langle \hat{\alpha}_{\vec{k}} \hat{\alpha}_{-\vec{q}}^{\dagger} \right\rangle_{\text{sq}} = \\ &= 2S\hbar^2 \left(|u_{\vec{k}}|^2 - |v_{\vec{k}}|^2 \right) \delta_{\vec{k}, -\vec{q}}. \end{aligned} \quad (\text{C7})$$

In the last line we dropped the resulting $\text{Im}(u_{\vec{k}} v_{\vec{k}})$ part, because $u_{\vec{k}}$ and $v_{\vec{k}}$ are real, as can be seen in the main text.

All other combinations of ladder operators can be calculated in a similar manner. The combination of the $-+$ operators yield the exact same result (except for the $-+$ crosscorrelator, which gets a minus sign), while the combination of the same operators ($++$ and $--$) are always equal to zero due to the absence of terms with the same number of annihilation and creation operators of the same mode.

From the expectation values of the $+-$ components we can determine the expectation values of xx , yy and xy combinations due to their relation to the ladder operator components via

$$\hat{S}_{\vec{k}}^x = \frac{1}{2} \left(\hat{S}_{\vec{k}}^+ + \hat{S}_{\vec{k}}^- \right), \quad \hat{S}_{\vec{k}}^y = \frac{1}{2i} \left(\hat{S}_{\vec{k}}^+ - \hat{S}_{\vec{k}}^- \right). \quad (\text{C8})$$

Again, a similar relation holds for the components of $\vec{Q}_{\vec{k}}$. From this expression we can calculate the correlators to be equal to the values in Eqs. (27), (28). The second part in the definition of the correlators will vanish, due to the fact, that each component is linear in the creation and annihilation operator of the magnons and therefore their expectation value will be zero.

b. z-Components

Left to show is, that the correlators including z-components will vanish. From the definition we get

$$\hat{S}_{\vec{k}}^z = \hbar \sqrt{\frac{2}{N}} \sum_{\vec{k}_1} \left(\hat{b}_{\vec{k}_1}^\dagger \hat{b}_{\vec{k}_1+\vec{k}} - \hat{a}_{\vec{k}_1}^\dagger \hat{a}_{\vec{k}_1+\vec{k}} \right), \quad (\text{C9})$$

$$\hat{Q}_{\vec{k}}^z = 2\hbar S \sqrt{\frac{N}{2}} \delta_{\vec{k},0} - \hbar \sqrt{\frac{2}{N}} \sum_{\vec{k}_1} \left(\hat{b}_{\vec{k}_1}^\dagger \hat{b}_{\vec{k}_1+\vec{k}} + \hat{a}_{\vec{k}_1}^\dagger \hat{a}_{\vec{k}_1+\vec{k}} \right). \quad (\text{C10})$$

As we only regard term up to order two in the annihilation and creation operators, it is obvious, that all products containing the z-component of the magnetization

will have a zero expectation value. For the expectation value of each z-component we have to consider

$$\begin{aligned} \left\langle \sum_{\vec{k}_1} a_{\vec{k}_1}^\dagger \hat{a}_{\vec{k}_1+\vec{k}} \right\rangle_{\text{sq}} &= \sum_{\vec{k}_1} |v_{\vec{k}_1}|^2 \delta_{\vec{k},0} \\ &= \left\langle \sum_{\vec{k}_1} b_{\vec{k}_1}^\dagger \hat{b}_{\vec{k}_1+\vec{k}} \right\rangle_{\text{sq}}, \end{aligned} \quad (\text{C11})$$

which implies $\left\langle \hat{S}_{\vec{k}}^z \right\rangle_{\text{sq}} = 0$ and

$$\left\langle \hat{Q}_{\vec{k}}^z \right\rangle_{\text{sq}} = 2\hbar \left(S \sqrt{\frac{N}{2}} - \sqrt{\frac{2}{N}} \sum_{\vec{k}_1} |v_{\vec{k}_1}|^2 \right) \delta_{\vec{k},0}. \quad (\text{C12})$$

From this it is a short calculation to show, that the correlator of the z-components of the Néel vector and of the z-components of the magnetization and the Néel vector vanishes. Further all products of other components (odd number of operators) with the z-components of the Néel vector (even number of operators) will also vanish if we take the expectation value.

-
- [1] G. Moore, “Cramming more components onto integrated circuits,” *Solid-State Circuits Newsletter, IEEE* **11**, 33–35 (2006).
- [2] M. Johnson and R. H. Silsbee, “Interfacial charge-spin coupling: Injection and detection of spin magnetization in metals,” *Phys. Rev. Lett.* **55**, 1790–1793 (1985).
- [3] X. Lou, C. Adelman, S. A. Crooker, E. S. Garlid, J. Zhang, K. S. M. Reddy, S. D. Flexner, C. J. Palmström, and P. A. Crowell, “Electrical detection of spin transport in lateral ferromagnet–semiconductor devices,” *Nature Physics* **3**, 197–202 (2007).
- [4] G. Binasch, P. Grünberg, F. Saurenbach, and W. Zinn, “Enhanced magnetoresistance in layered magnetic structures with antiferromagnetic interlayer exchange,” *Phys. Rev. B* **39**, 4828–4830 (1989).
- [5] Peter M. Levy, Shufeng Zhang, and Albert Fert, “Electrical conductivity of magnetic multilayered structures,” *Phys. Rev. Lett.* **65**, 1643–1646 (1990).
- [6] M. Julliere, “Tunneling between ferromagnetic films,” *Physics Letters A* **54**, 225–226 (1975).
- [7] A. V. Chumak, V. I. Vasyuchka, A. A. Serga, and B. Hillebrands, “Magnon spintronics,” *Nature Physics* **11**, 453–461 (2015).
- [8] R. Lebrun, A. Ross, S. A. Bender, A. Qaiumzadeh, L. Baldrati, J. Cramer, A. Brataas, R. A. Duine, and M. Kläui, “Tunable long-distance spin transport in a crystalline antiferromagnetic iron oxide,” *Nature* **561**, 222–225 (2018).
- [9] L. J. Cornelissen, J. Liu, R. A. Duine, J. Ben Youssef, and B. J. van Wees, “Long-distance transport of magnon spin information in a magnetic insulator at room temperature,” *Nature Physics* **11**, 1022–1026 (2015).
- [10] Freeman J. Dyson, “General Theory of Spin-Wave Interactions,” *Phys. Rev.* **102**, 1217–1230 (1956).
- [11] C. Kittel, *Einführung in die Festkörperphysik* (De Gruyter, Berlin, 2013).
- [12] W. Nolting and A. Ramakanth, *Quantum Theory of Magnetism* (Springer Berlin Heidelberg, Berlin, Heidelberg, 2009).
- [13] F. Bloch, “Zur Theorie des Ferromagnetismus,” *Zeitschrift für Physik* **61**, 206–219 (1930).
- [14] B. N. Brockhouse, “Scattering of Neutrons by Spin Waves in Magnetite,” *Phys. Rev.* **106**, 859–864 (1957).
- [15] K. S. Novoselov, D. Jiang, F. Schedin, T. J. Booth, V. V. Khotkevich, S. V. Morozov, and A. K. Geim, “Two-dimensional atomic crystals,” *Proc. Natl. Acad. Sci. USA* **102**, 10451–10453 (2005).
- [16] K. S. Novoselov, A. K. Geim, S. V. Morozov, D. Jiang, Y. Zhang, S. V. Dubonos, I. V. Grigorieva, and A. A. Firsov, “Electric field effect in atomically thin carbon films,” *Science* **306**, 666–669 (2004).
- [17] Alexander S. Mayorov, Roman V. Gorbachev, Sergey V. Morozov, Liam Britnell, Rashid Jalil, Leonid A. Ponomarenko, Peter Blake, Kostya S. Novoselov, Kenji Watanabe, Takashi Taniguchi, and A. K. Geim, “Micrometer-Scale Ballistic Transport in Encapsulated Graphene at Room Temperature,” *Nano Letters* **11**, 2396–2399 (2011).
- [18] Kin Fai Mak, Changgu Lee, James Hone, Jie Shan, and Tony F. Heinz, “Atomically Thin MoS₂: A New Direct-Gap Semiconductor,” *Phys. Rev. Lett.* **105**, 136805 (2010).
- [19] B. Radisavljevic, A. Radenovic, J. Brivio, V. Giacometti, and A. Kis, “Single-layer MoS₂ transistors,” *Nature Nan-*

- otechnology **6** (2011).
- [20] K. S. Novoselov, A. Mishchenko, A. Carvalho, and A. H. Castro Neto, “2D materials and van der Waals heterostructures,” *Science* **353**, 6298 (2016).
- [21] C. Elias, P. Valvin, T. Pelini, A. Summerfield, C. J. Mellor, T. S. Cheng, L. Eaves, C. T. Foxon, P. H. Beton, S. V. Novikov, B. Gil, and G. Cassabois, “Direct band-gap crossover in epitaxial monolayer boron nitride,” *Nature Communications* **10** (2019).
- [22] S. J. Haigh, A. Gholinia, R. Jalil, S. Romani, L. Britnell, D. C. Elias, K. S. Novoselov, L. A. Ponomarenko, A. K. Geim, and R. Gorbachev, “Cross-sectional imaging of individual layers and buried interfaces of graphene-based heterostructures and superlattices,” *Nature Materials* **11**, 764–767 (2012).
- [23] A. K. Geim and I. V. Grigorieva, “Van der Waals heterostructures,” *Nature* **499**, 419–425 (2013).
- [24] Cheng Gong, Lin Li, Zhenglu Li, Huiwen Ji, Alex Stern, Yang Xia, Ting Cao, Wei Bao, Chenzhe Wang, Yuan Wang, Z. Q. Qiu, R. J. Cava, Steven G. Louie, Jing Xia, and Xiang Zhang, “Discovery of intrinsic ferromagnetism in two-dimensional van der Waals crystals,” *Nature* **546**, 265–269 (2017).
- [25] Bevin Huang, Genevieve Clark, Efrén Navarro-Moratalla, Dahlia R Klein, Ran Cheng, Kyle L Seyler, Ding Zhong, Emma Schmidgall, Michael A McGuire, David H Cobden, Wang Yao, Di Xiao, Pablo Jarillo-Herrero, and Xiaodong Xu, “Layer-dependent ferromagnetism in a van der Waals crystal down to the monolayer limit,” *Nature* **546**, 270–273 (2017).
- [26] M. Gibertini, M. Koperski, A.F. Morpurgo, and K.S. Novoselov, “Magnetic 2D materials and heterostructures,” *Nature Nanotechnology* **14**, 408–419 (2019).
- [27] K. S. Burch, D. Mandrus, and J.-G. Park, “Magnetism in two-dimensional van der Waals materials,” *Nature* **563**, 47–52 (2018).
- [28] S. O. Demokritov, V. E. Demidov, O. Dzyapko, G. A. Melkov, A. A. Serga, B. Hillebrands, and A. N. Slavin, “Bose–Einstein condensation of quasi-equilibrium magnons at room temperature under pumping,” *Nature* **443**, 430–433 (2006).
- [29] Andreas Rückriegel and Peter Kopietz, “Rayleigh-Jeans Condensation of Pumped Magnons in Thin-Film Ferromagnets,” *Phys. Rev. Lett.* **115**, 157203 (2015).
- [30] A. Kamra and W. Belzig, “Super-poissonian shot noise of squeezed-magnon mediated spin transport,” *Phys. Rev. Lett.* **116**, 146601 (2016).
- [31] A. Kamra and W. Belzig, “Spin pumping and shot noise in ferrimagnets: Bridging ferro- and antiferromagnets,” *Phys. Rev. Lett.* **119**, 197201 (2017).
- [32] A. Roldán-Molina, Alvaro S. Nunez, and R. A. Duine, “Magnonic Black Holes,” *Phys. Rev. Lett.* **118**, 061301 (2017).
- [33] A. Kamra, E. Thingstad, G. Rastelli, R. A. Duine, A. Brataas, W. Belzig, and A. Sudbø, “Antiferromagnetic magnons as highly squeezed Fock states underlying quantum correlations,” *Phys. Rev. B* **100**, 174407 (2019).
- [34] A. Kamra, W. Belzig, and A. Brataas, “Magnon-squeezing as a niche of quantum magnonics,” *Applied Physics Letters* **117**, 090501 (2020).
- [35] Ji Zou, Se Kwon Kim, and Yaroslav Tserkovnyak, “Tuning entanglement by squeezing magnons in anisotropic magnets,” *Phys. Rev. B* **101**, 014416 (2020).
- [36] Christopher Gerry and Peter Knight, *Introductory Quantum Optics* (Cambridge University Press, 2004).
- [37] A. Kamra and W. Belzig, “Magnon-mediated spin current noise in ferromagnet | nonmagnetic conductor hybrids,” *Phys. Rev. B* **94**, 014419 (2016).
- [38] A. Kamra, U. Agrawal, and W. Belzig, “Noninteger-spin magnonic excitations in untextured magnets,” *Phys. Rev. B* **96**, 020411(R) (2017).
- [39] Lu-Ming Duan, G. Giedke, J. I. Cirac, and P. Zoller, “Inseparability criterion for continuous variable systems,” *Phys. Rev. Lett.* **84**, 2722–2725 (2000).
- [40] T. Holstein and H. Primakoff, “Field Dependence of the Intrinsic Domain Magnetization of a Ferromagnet,” *Phys. Rev.* **58**, 1098–1113 (1940).
- [41] H. P. Robertson, “The Uncertainty Principle,” *Phys. Rev.* **34**, 163–164 (1929).
- [42] Vahid Azimi Mousolou, Yuefei Liu, Anders Bergman, Anna Delin, Olle Eriksson, Manuel Pereiro, Danny Thonig, and Erik Sjöqvist, “Magnon-magnon entanglement and its detection in a microwave cavity,” (2021), [arXiv:2106.06862](https://arxiv.org/abs/2106.06862) [quant-ph].